

Structural Characterization of Valinomycin and Nonactin at the Air–Solution Interface by Grazing Incidence X-ray Diffraction

Hanna Rapaport,^{*,†} Ivan Kuzmenko,[†] Kristian Kjaer,[‡] Paul Howes,[‡]
Wim Bouwman,[‡] Jens Als-Nielsen,[§] Leslie Leiserowitz,^{*,†} and Meir Lahav^{*,†}

Contribution from the Department of Materials and Interfaces, Weizmann Institute of Science, Rehovot 76100, Israel, Department of Solid State Physics, Risø National Laboratory, DK-4000 Roskilde, Denmark, and Niels Bohr Institute, H. C. Ørsted Laboratory, Universitetsparken 5, DK-2100 Copenhagen, Denmark

Received May 2, 1997[⊗]

Abstract: Grazing incidence X-ray diffraction (GID) has been applied to the study of structural characteristics of two-dimensional crystallites of the ionophores valinomycin (VM) and nonactin (NA) when complexed with various cations at the air–solution interface. The VM complexes assume a bracelet shape that packs in a two-dimensional hexagonal unit cell. Other crystalline phases were formed on potassium iodide and barium perchlorate solutions. The presence of particular lipids induced ordered stacking of VM–potassium chloride complexes into three to four layers. NA packs in a pseudotetragonal unit cell on solutions of NH₄SCN and KSCN. Upon compression of the NA–NH₄SCN film, crystallites seven to eight layers thick were detected and the GID data enabled the determination of the structure. The tendency of these complexed ionophores to form multilayer crystallites at interfaces may have bearing on ion transport through membranes, via stacking.

Introduction

Ionophores are capable of selectively carrying ions across natural and artificial membranes. The ion transport is associated with structural reorganization that takes place inside the membrane and at its interface.¹ Among the most frequently studied ionophores are valinomycin (VM), which is highly selective to binding of potassium and rubidium cations,¹ and nonactin (NA), which complexes efficiently with ammonium, potassium, and sodium cations. VM is a cyclic dodecadep-sipeptide with the molecular formula *cyclo*–[(L-Val-D-Hyv-D-Val-L-Lac)₃–], where D-Hyv is D- α -hydroxyisovaleric acid and L-Lac is L-lactic acid. NA is a macrotetrolide formed by four nonactinic acid units with alternating chirality. Physicochemical studies, aimed at revealing the mechanism of ion transport by ionophores, have been the major source of information regarding the conformations adopted by the ionophores in different solvents and in the presence of ions.² X-ray crystal structure analyses have provided details of several conformations of the cation complexed ionophores and of their free forms.^{3–5} Few reports have focused on the investigation of these compounds in an environment resembling that of a membrane, such as monolayers at interfaces.^{6–10} Structural studies of model membranes containing ionophores, as films at air–solution

Table 1. Results of Bragg Peak Analysis for the VM and NA Ionophores on Different Subphases^a

film	subphase	<i>a</i> [Å]	<i>b</i> [Å]	γ [deg]	<i>z</i>	<i>A</i> [Å ²]
VM	KCl	13.8	13.8	120	1	164.9
	KBr	13.7	13.7	119.5	1	162.5
	KI ^b	13.8	13.8	120	1	164.9
	RbCl	13.9	13.9	120	1	167.3
	RbBr	13.8	13.8	120	1	164.9
VM:C ₁₇ COOH ^c	KCl	13.7	13.7	120	1	162.5
VM:DPPA ^c	KCl	13.8	13.8	120	1	164.9
VM	Ba(ClO ₄) ₂	29.5	16.3	90	2	241.3
NA	NH ₄ SCN, ^c KSCN	15.3	15.7	90	2	120.1

^a All subphases were 1 M in concentration. *a* and *b* are the dimensions of the unit cell axes. γ is the angle between the *a* and *b* axes. *z* is the number of molecules in the *ab* plane. *A* is the area per molecule = $ab(\sin\gamma)/z$. ^b This crystalline form was observed upon compression of the film to the area 110 Å²/molecule; the other phases of the VM/KI system could not be assigned (see text). ^c Multilayers were detected (see text).

interfaces, may contribute to the elucidation of the processes that take place at the hydrophilic/hydrophobic interface and inside the two-dimensional environment of the long-chain lipids. The design of ionoselective electrodes and sensors utilizing ionophores may also benefit by this type of study.

Here we report the structural features of two-dimensional films of VM and NA at air–aqueous solution interfaces as revealed by grazing incidence X-ray diffraction (GID). We have investigated the effect of various types of ions in solution and that of a lipid matrix on the 2D crystallization of the ionophores.

Experimental Section

Valinomycin, nonactin, L-dipalmitoyl phosphatidic acid, and stearic acid, of the highest purity available, were obtained from SIGMA. The film-forming compounds were dissolved in chloroform (MERCK, analytical grade). All salts for the preparation of subphase solutions were also purchased from SIGMA. The 2D films measured by GID were also studied by surface–pressure area isotherms.

Grazing Incidence X-ray Diffraction (GID) Experiments. A detailed description of the GID method regarding amphiphilic molecules is given in ref 12. The grazing incidence X-ray diffraction experiments were performed at the undulator BW1 beam line on a liquid surface diffractometer at the Hasylab synchrotron source (Hamburg). A

[†] Weizmann Institute of Science.

[‡] Risø National Laboratory.

[§] Niels Bohr Institute.

[⊗] Abstract published in *Advance ACS Abstracts*, October 15, 1997.

(1) Ovchinnikov, Y. A.; Ivanov, V. T., Shkrob, A. M. *Membrane Active Complexones*; Elsevier: Amsterdam, 1974.

(2) Ovchinnikov, Y. A. *Eur. J. Biochem.* **1979**, *94*, 321.

(3) Dobler, M. *Ionophores and Their Structures*; John Wiley & Sons: New York, 1981.

(4) Langs, D. A.; Blessing, R. H.; Duax, W. L. *J. Peptide Protein Res.* **1992**, *39*, 291.

(5) Devarajan, S.; Vijayan, M.; Easwaran, K. R. K. *Int. J. Peptide Protein Res.* **1984**, *23*, 324.

(6) Kemp, G.; Wenner, C. E. *Biochim. Biophys. Acta* **1972**, *282*, 1.

(7) Zaitsev, S. Y.; Zubov, V. P.; Mobius, D. *Biochim. Biophys. Acta* **1993**, *1148*, 191.

(8) Pathirana, S.; Neely, W. C.; Myers, L. J.; Vodyanoy, V. *Langmuir* **1992**, *8*, 1984.

(9) Vodyanoy, V.; Pathirana, S.; Neely, W. C. *Langmuir* **1994**, *10*, 1354.

(10) Reis, H. E.; Swift, H. S. *J. Colloid Interface Sci.* **1978**, *64*, 111.

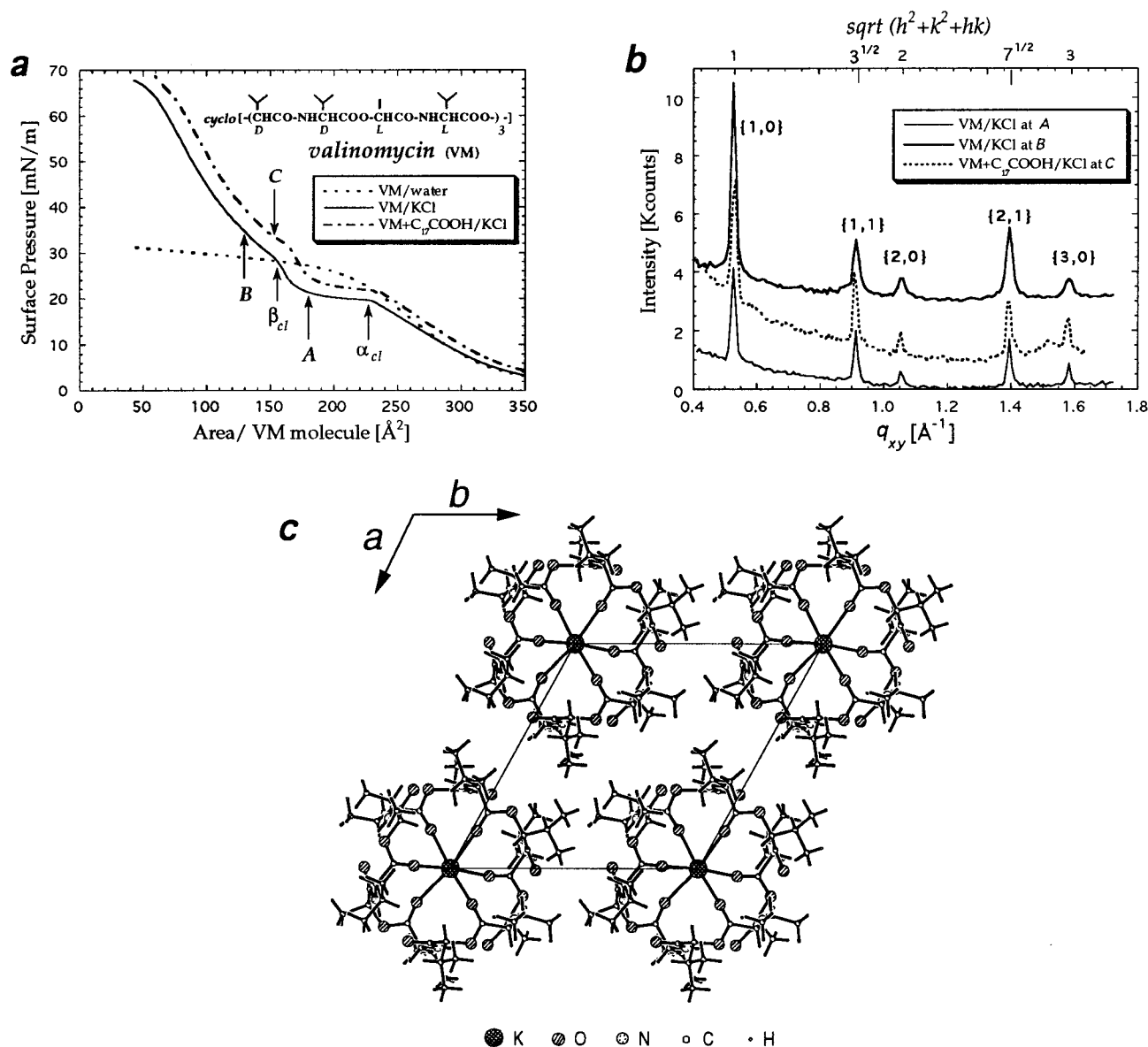


Figure 1. (a) Surface pressure–area isotherms of VM at 5 °C, on pure water (dotted line), on 1 M KCl solution subphase (solid line), and in an equimolar mixture with stearic acid on 1 M KCl solution (dash-dot line). Kinks in VM–KCl isotherms, similar to previously reported data,^{6,7} are labeled by α_{cl} and β_{cl} . Arrows labeled A, B, and C denote the state of the film where GID measurements were performed. (b) The GID patterns (see Methods) of the VM–KCl system, measured at 180 (A, thin line) and 130 Å²/molecule (B, thick line). The GID pattern of the 1:1 molar mixture of VM and C₁₇COOH on 1 M KCl solution (C, dotted line). Bragg peaks are assigned by the $\{h,k\}$ indices of the 2D hexagonal lattice. (c) The molecular packing in the 2D hexagonal unit cell ($a = b = 13.8$ Å, $\gamma = 120^\circ$) of the VM–potassium cation complex, assuming the bracelet-like shape¹³ as in the C222₁ polymorph.

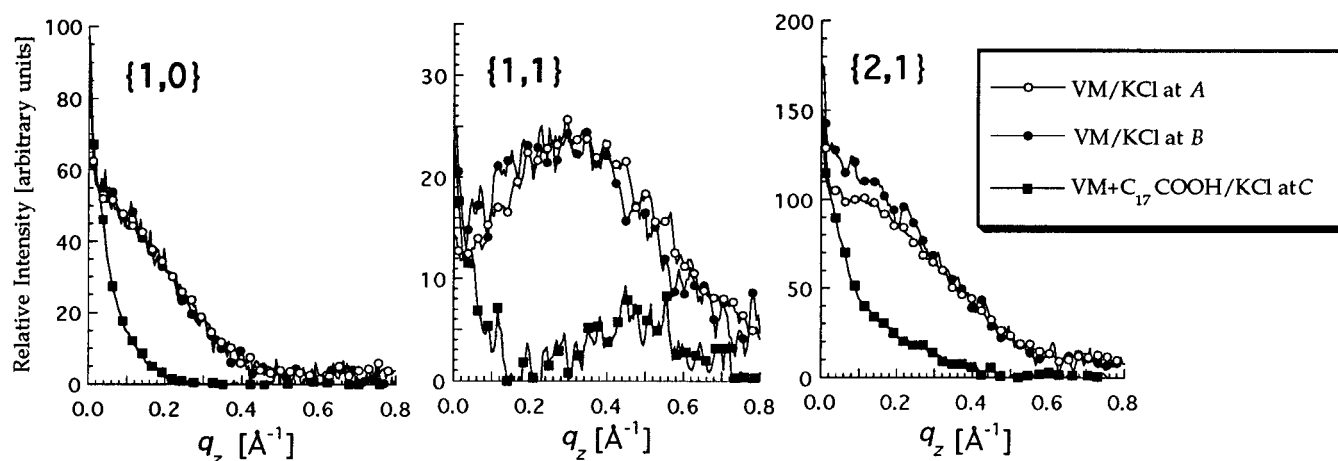
monochromated X-ray beam was adjusted to strike the liquid surface at an incident angle ($\alpha \approx 0.85\alpha_c$ where α_c is the critical angle for the total external reflection) that maximizes surface sensitivity. The dimensions of the footprint of the incoming X-ray beam on the liquid surface were approximately 5×50 mm². GID signals are obtained from 2D crystallites azimuthally randomly oriented. The scattered intensity was collected by means of a position-sensitive detector (PSD) that intercepts photons over the range $0.0 \leq q_z \leq 0.9$ Å⁻¹, where q_z is the vertical component of the X-ray scattering vector, $\approx (2\pi/\lambda) \sin \alpha_i$, α_i being the angle between the horizon and the diffracted beam. Measurements were performed by scanning over a range along the horizontal scattering vector q_{xy} ($\approx 4\pi \sin \theta_{xy}/\lambda$, where $2\theta_{xy}$ is the angle between the incident and diffracted beam projected onto the horizontal plane) and over the whole q_z window of the PSD. These diffraction data are represented in two ways: The grazing incidence diffraction pattern shows the Bragg peak intensity profiles $I(q_{xy})$ obtained by integrating the whole q_z intensity for any q_{xy} along the measured range. Bragg rod profiles show the scattered intensity $I(q_z)$ in channels along the PSD, integrated over the whole range in q_{xy} for a Bragg peak.

The q_{xy} positions of the Bragg peaks yield the lattice repeat distances $d = 2\pi/q_{xy}$, which may be indexed by the two indices h,k to yield the unit cell. The full width at half maximum (FWHM) of the Bragg peaks in q_{xy} units yields the 2D crystalline coherence length¹¹ associated with the h,k reflection. The width of the Bragg rod profile along q_z gives a measure of the height of the crystalline film,¹² $\approx 0.9(2\pi)/\Delta q_z$. The intensity at a particular value of q_z in a Bragg rod is determined by the square of the molecular structure factor $|F_{hk}(q_z)|^2$, thus allowing its evaluation according to an atomic model of the molecules. Unlike previous structure determinations of crystalline films of amphiphilic molecules,¹² the molecular structures and packing arrangements described here are more complex. For structure determination of these systems from GID data, we made use of known three-dimensional crystal structures, followed by minor adjustments such as molecular orientation and counterion position.

(11) Guinier, A. *X-ray diffraction*; Freeman: San Francisco, 1968.

(12) Als-Nielsen, J.; Jacquemain, D.; Kjaer, K.; Leveiller, F.; Lahav, M.; Leiserowitz, L. *Phys. Rep.* **1994**, *246*, 251.

a



b

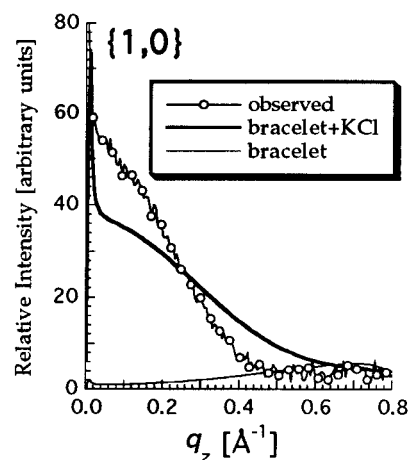


Figure 2. (a) Observed Bragg rods of the $\{1,0\}$, $\{1,1\}$, and $\{2,1\}$ reflections of the VM–KCl system, measured at *A* (open circles connected by a line), at *B* (solid circles connected by a line), and at *C* (solid squares connected by a line). The FWHM of the rods at *A* and *B* ($\Delta q_z = 0.4\text{--}0.5 \text{ \AA}^{-1}$) indicate a film thickness of 11–14 Å, and thus a monolayer, whereas for VM + C₁₇COOH/KCl the FWHM of these Bragg rods at *C* ($\Delta q_z = 0.14\text{--}0.16 \text{ \AA}^{-1}$) points to 3–4 layers. (b) The $\{1,0\}$ Bragg rod of the VM 2D lattice that includes the bracelet and the KCl ions, as derived by atomic structure factor calculations (thick line). The molecular bracelet itself contributed very little to the calculated intensity of the Bragg rod $\{1,0\}$ (thin line). The observed $\{1,0\}$ Bragg rod (open circles) is also displayed for comparison.

Results and Discussion

The GID measurements of VM on pure water and on concentrated solutions of KCl, KBr, KI, RbCl, and RbBr solutions were performed at various points along the surface pressure–area (π –*A*) isotherms, and the patterns observed are similar to previously reported data.^{6,7} No diffraction was observed from VM films on pure water, whereas VM on all the salt solutions (except for KI, which will be described below), upon compression, resulted in similar diffraction patterns (Table 1).

Here we first focus on the VM–KCl system. The isotherm of VM on KCl solution⁶ shown in Figure 1a exhibits two kinks α_{cl} and β_{cl} separated by a plateau. This film diffracted only when compressed beyond the point α_{cl} , implying the transition from a disordered to a crystalline phase. All the Bragg peaks of the diffraction pattern *A* (Figure 1b, at 180 \AA^2) were indexed in terms of a two-dimensional (2D) hexagonal unit cell, $a = b = 13.8 \text{ \AA}$, $\gamma = 120^\circ$ with a molecular area $a^2 \sin \gamma = 164.9 \text{ \AA}^2$ (Table 1). These dimensions are almost equal to those of the *ab* plane in the three-dimensional (3D) trigonal crystal form¹³

of valinomycin–KI ($a = b = 13.7 \text{ \AA}$, $c = 25.7 \text{ \AA}$, $\gamma = 120^\circ$). Consequently, complexed valinomycin molecules at the air–solution interface assume a bracelet-like shape (Figure 1c) similar to that found in the 3D crystal. This bracelet is composed of a core formed by six carbonyl oxygens coordinated to the central cation, and a hydrophobic surface at the external boundary of the molecule, with 3-fold symmetry conducive to favorable lateral packing of the molecules.

The calculated thickness of the film 11–14 Å, as derived from the width of the Bragg rods (Figure 2a, circles), fits the interlayer spacing of 12.8 Å in the 3D crystal structure, and therefore implies a monolayer. Making use of atomic structure factor calculations based on the model given in Figure 1c, we found that the molecular bracelet itself contributed very little to the calculated intensity of the Bragg rod $\{1,0\}$ (thin line in Figure 2b). Only upon introduction of the K⁺ ion, and the Cl[−] counterion when placed at a distance of 5 Å directly below the cation, did we obtain a far more reasonable fit to the $\{1,0\}$ Bragg

(13) Neupert-Laves, K.; Dobler, M. *Helv. Chim. Acta* **1975**, *58*, 432.

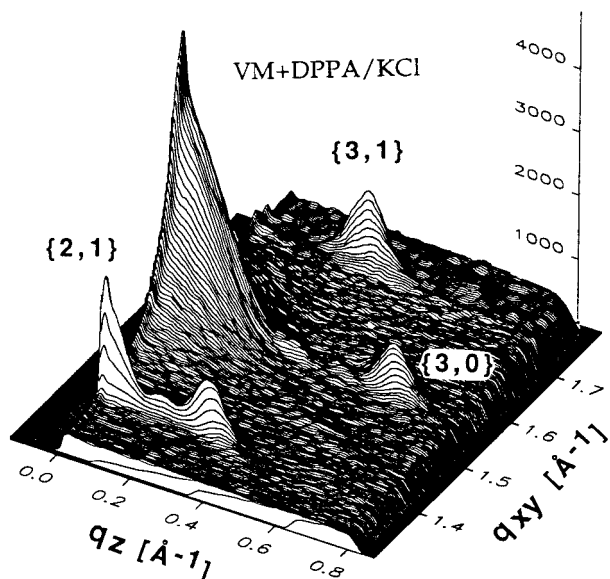


Figure 3. The two-dimensional intensity pattern $I(q_{xy}, q_z)$ of the 1:1 molar mixture of VM and DPPA obtained at 45 mN/m. The Bragg rod peak at $q_{xy} = 1.55 \text{ \AA}^{-1}$ arises from DPPA, and that at $q_{xy} = 1.39, 1.56, 1.74 \text{ \AA}^{-1}$ from multilayers of VM–KCl.

rod (thick line in Figure 2b). We stress that the intensity profiles of the Bragg rods are to an extent dependent upon the conformation and thus positions of the isopropyl groups, which we were not able to ascertain.

On further compression of the VM–KCl film to a surface area of $130 \text{ \AA}^2/\text{molecule}$ the GID pattern remained unchanged (cf. curves A and B in Figure 1b and curves delineated by open and solid circles in Figure 2a), thus on crossing the kink β_{cl} , the crystal structure remained the same and no crystalline multilayer formed. The relative intensities at A and at B (Figure 1b) are proportional to the decrease in the area per molecule, according to the lever rule, and therefore the plateau between kinks α_{cl} and β_{cl} corresponds to a transition between a disordered and an ordered monolayer.

Studies of the effect of a membrane-like matrix on the behavior of VM were performed with a 1:1 molar mixture of VM and stearic acid ($C_{17}COOH$) on KCl solution. The isotherm has a shape similar to that of pure VM–KCl (Figure 1a, dash-dot line). Likewise, diffraction signals were obtained only when the film was compressed to a state beyond the first kink α_{cl} . The GID pattern (Figure 1b, dotted line) indicates formation of the 2D hexagonal phase composed of VM–KCl crystallites (Table 1) and a minor amount of crystalline $C_{17}COOH$ (giving rise to the small Bragg reflection at $q_z \approx 1.55 \text{ \AA}^{-1}$), from which we deduce that the two components are phase separated. The pronounced decrease in the widths of the Bragg rod profiles of the hexagonal lattice (Figure 2a, squares), as compared with those of pure VM on KCl (Figure 2a, circles), points to formation of crystallites three to four layers thick. Obviously, the presence of $C_{17}COOH$ induced interlayer ordering of VM–KCl. A similar behavior was observed for a 1:1 molar mixture of VM and dipalmitoyl phosphatidic acid (DPPA) (Figure 3 and Table 1).

The π –A isotherm of the VM–KI system (Figure 4a) shows two kinks (α_l and β_l). GID peaks were observed only when the monolayer was compressed beyond the first kink α_l , in a manner akin to the previously-described systems. The diffraction pattern of VM–KI (thick line in Figure 4b), which is very different from that of the hexagonal phase of VM–KCl, was measured at 320 \AA^2 and did not change upon compression down to 165 \AA^2 . The various Bragg rods exhibit differences in the

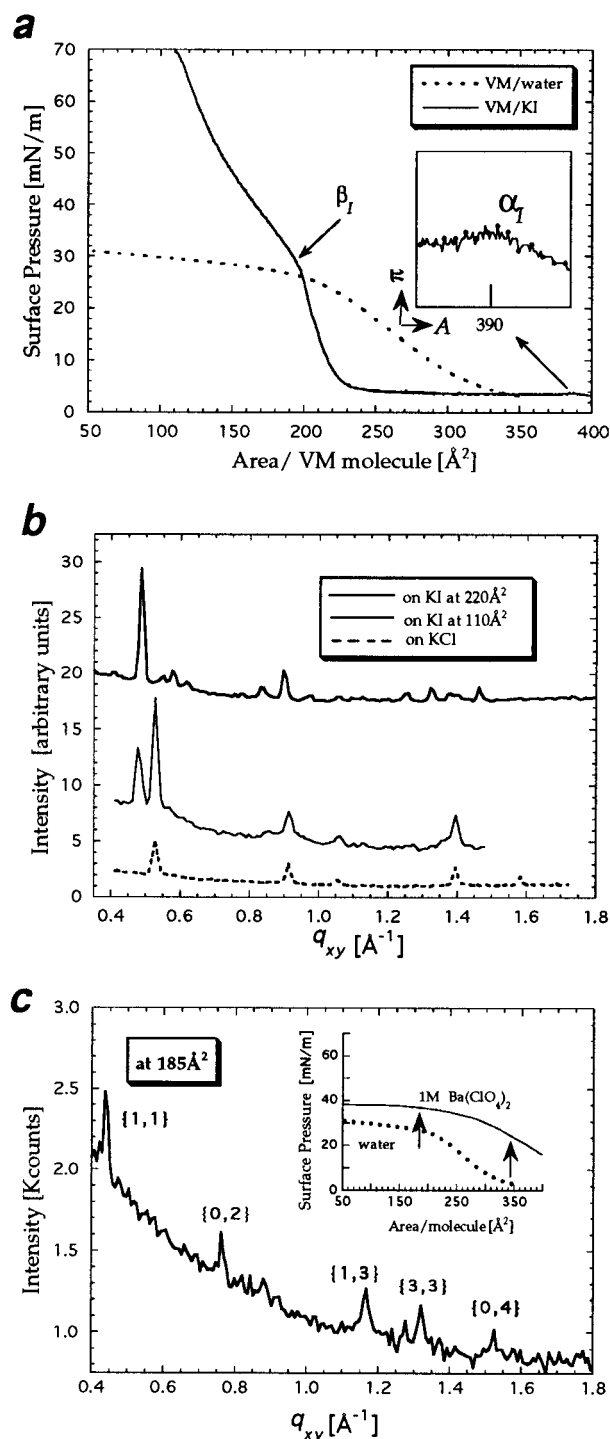


Figure 4. (a) Surface pressure–area isotherms of VM at $5 \text{ }^\circ\text{C}$, on pure water (dotted line) and on 1 M KI solution subphase (solid line), showing kinks labeled α_l and β_l in the isotherm curve, similar to previously reported data.^{6,7} (b) GID pattern of VM film on 1 M KI solution, which was measured at 220 \AA^2 (thick line); similar patterns were obtained in the region 320 – 165 \AA^2 . The GID pattern at the nominal area per molecule of 110 \AA^2 (thin line) consists of the peak at $q_{xy} = 0.48 \text{ \AA}^{-1}$, which is slightly shifted with respect to the previous scan. The four other Bragg peaks of this scan belong to the pure hexagonal phase as in the VM–KCl system (shown for comparison by a dashed line). (c) GID diffraction pattern of VM on 1 M $Ba(ClO_4)_2$ solution measured at an area per molecule of 185 \AA^2 . Bragg peaks are assigned by the $\{h,k\}$ indices of the 2D rectangular unit cell. The inset shows surface pressure–area isotherms, measured at $5 \text{ }^\circ\text{C}$, on 1 M solution of $Ba(ClO_4)_2$ (solid line) and on water (dotted line).

number of intensity modulations and FWHM, denoting more than one crystalline phase. This observation is in agreement

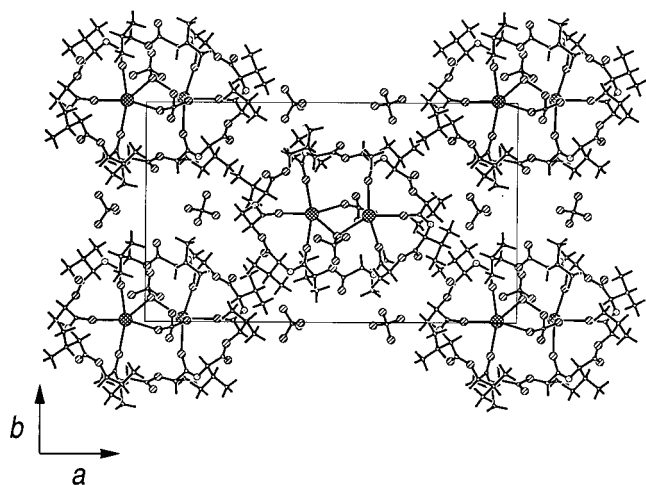


Figure 5. The proposed molecular packing of VM–Ba(ClO₄)₂ complex, in the 2D rectangular unit cell, at the air–solution interface, which is essentially the *ab* plane of the 3D crystal structure.⁵

with the fact that VM–KI yields six polymorphic 3D crystals.¹³ Indeed we were not able to index all the Bragg peaks by assuming a single phase, nor by combinations of the dimensions of the reported 3D crystals. Polymorphism is also made manifest upon further compression of the film to 110 Å² (see the thin line in Figure 4b), where Bragg peaks signaling the pure hexagonal phase, as in the VM–KCl system, appeared

(Table 1). Intercalated solute molecules or differences in the VM conformation may give rise to the 2D polymorphism.

The above observations led us to explore whether VM at the air–solution interface may be ordered in a shape different than the bracelet. In the 3D crystal of VM complexed with barium perchlorate,⁵ the backbone of the molecules is elliptical in shape, resulting in a cross-sectional area of 240 Å². The π –*A* isotherm of VM on Ba(ClO₄)₂ displays a gradual increase in pressure followed by a plateau. GID scans on the slope of the isotherm, at 345 Å², yielded no diffraction signal whereas upon compression to the plateau region at 185 Å², Bragg peaks were observed (Figure 4c). We were able to assign to these data a rectangular unit cell, *a* = 29.5 Å *b* = 16.3 Å, the area per molecule of *ab*/2 = 241.3 Å² (Table 1), which is similar in dimensions to the *ab* lattice plane (*a* = 28.30 Å, *b* = 16.94 Å) of the 3D crystal structure (Figure 5). This result demonstrates that cation-bound valinomycin at the air–aqueous solution interface may adopt shapes other than the bracelet-like form.

Nonactin (NA) binds selectively to ammonium, potassium, and sodium cations. The π –*A* isotherm of NA on pure water (Figure 6a) shows a monotonic rise in surface pressure; similar isotherms were observed on KCl and on NH₄Cl solution subphases. NA on NH₄SCN and KSCN solutions displays isotherms with a distinct kink (Figure 6a). In keeping with the differences in isotherm shape, NA on pure water and on KCl solution yielded no GID signals, whereas on both KSCN and NH₄SCN solutions, the appearance of an almost identical GID

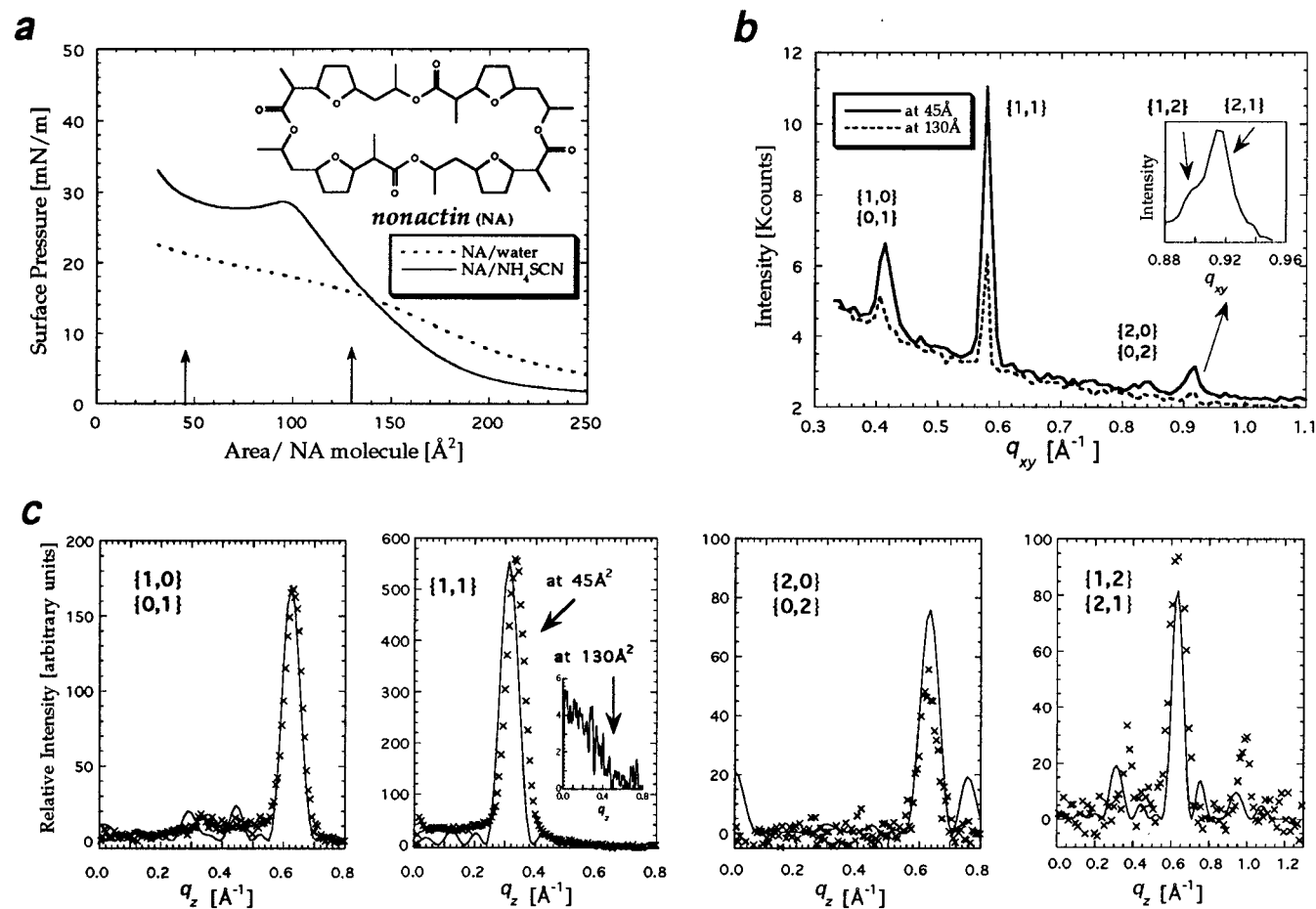


Figure 6. (a) Surface pressure–area isotherms, measured at 5 °C, of NA on 1 M NH₄SCN solution subphase (solid line) and on pure water (dotted line). The arrows denote the state of the film at which GID measurements were made (130 and 45 Å²/molecule). (b) GID pattern of NA on 1 M NH₄SCN solution, measured at 130 (dotted line) and 45 Å²/molecule (solid line). The Bragg peaks could be fitted to a pseudotetragonal cell, *a* = 15.3 Å, *b* = 15.7 Å, γ = 90°. The deviation from pure tetragonal symmetry was made evident from the peak doublet at *q*_{xy} = 0.92 Å^{−1} corresponding to the Bragg peaks {1,2} and {2,1}, shown in the inset. (c) Observed (crosses) and calculated (solid line) Bragg rods for the NA–NH₄SCN 2D unit cell represented in Figure 7.

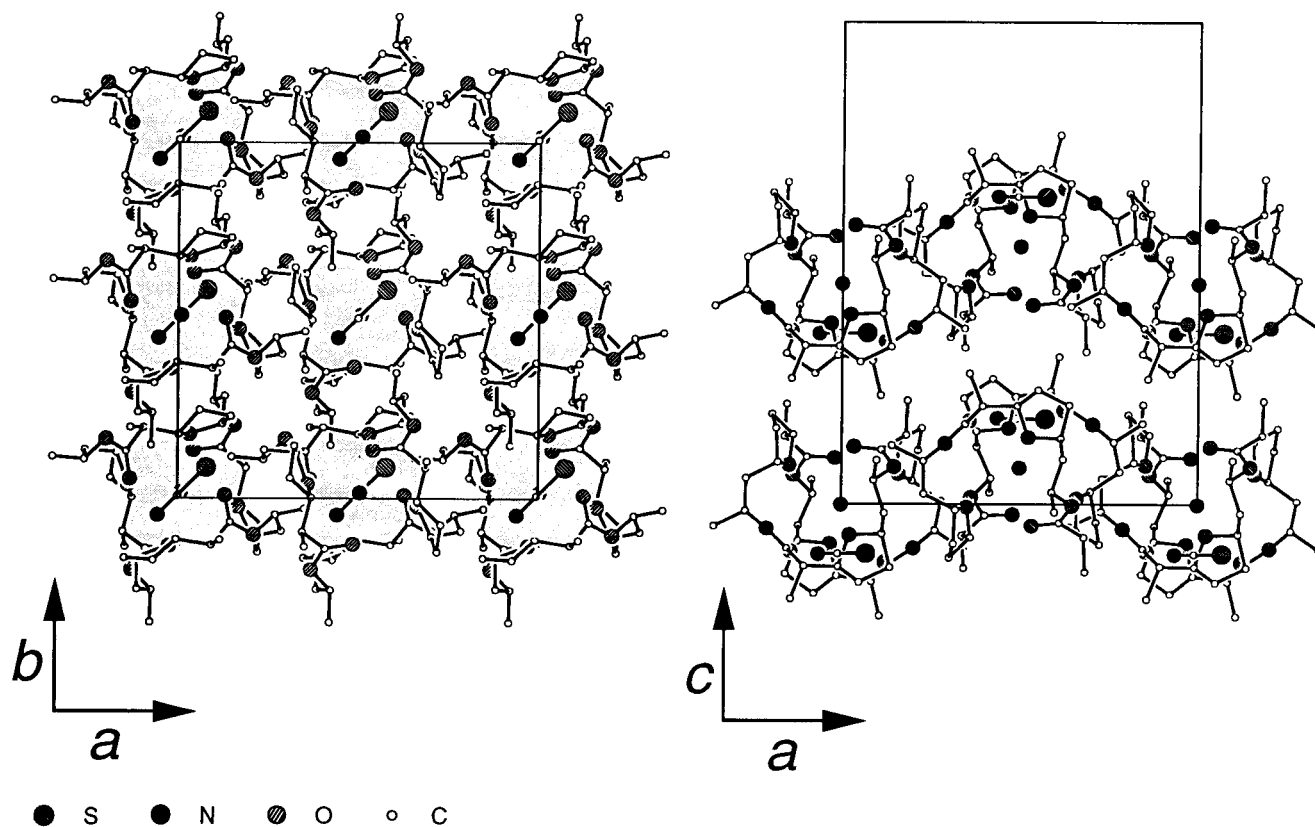


Figure 7. Model of the molecular packing arrangement of NA–NH₄SCN crystallites, showing the top and side views of two layers. The crystal structure was generated with the help of the CERIUSt² software computational package.

pattern denoted formation of 2D crystallites of like arrangement. Bragg peaks from a film of NA–NH₄SCN were already observed at 130 Å²/molecule, well before the kink. The {1,1} Bragg rod obtained at 130 Å²/molecule (see Figure 6c, the inset of that Bragg rod) displays a fwhm of 0.58 Å⁻¹ that indicates a film ~10 Å thick and thus a crystalline monolayer. Compression to 45 Å² produced not only an enhancement in intensity of Bragg peaks (Figure 6b) but also a transition from monolayer to multilayer, manifested by the reduction in the FWHM of the Bragg rods (Figure 6c). The diffraction pattern at 45 Å² could be indexed according to a pseudotetragonal cell, $a = 15.3$ Å, $b = 15.7$ Å, $c = 19.6$ Å⁻¹, $\gamma = 90^\circ$ (Table 1), in keeping with the 4 symmetry of the molecule and very similar to that of the *ab* plane of the known 3D crystal structure.³ The 0.32-Å⁻¹ separation along q_z , between neighboring Bragg rod modulations, corresponds to a lattice repeat of 19.6 Å, and thus an interlayer spacing of 9.8 Å. The FWHM of these Bragg rods (0.068 to 0.080 Å⁻¹) yielded a film thickness of 7–8 layers.

The derived dimensions of the *ab* unit cell and the interlayer spacing of the 2D lattice compare very well with the cell dimensions of the 3D crystal structures of the NH₄⁺, Na⁺, and K⁺ complexes of NA. All these crystals are essentially isostructural although appearing in different space groups with the following average dimensions $a = 15.21(18)$ Å, $b = 15.56(30)$ Å, $\gamma = 90.3^\circ(6^\circ)$ (cf. $a = 15.3$ Å, $b = 15.7$ Å, $\gamma = 90.0^\circ$ of the 2D lattice obtained at the air–solution interface). We have therefore assumed that the multilayer of NA at the air–aqueous solution interface adopts a similar packing arrangement. The model of the 2D unit cell that was constructed (Figure 7) contains two molecules related by an *n* glide parallel to the *ab* plane. The interlayer arrangement in the model is achieved by offsetting the layers along the diagonal $1/2(b + c)$ by *A*-centering to yield space group *A11a*. The presence of an *n* glide and *A* centering are substantiated by the absence of observed intensity

modulations of the type $h + k = 2n + 1$ for the *hk0* reflections and $k + l = 2n + 1$ for *hkl* reflections. X-ray structure factor analysis of the refined model of the 2D crystallites unit cell resulted in good agreement between the calculated and the observed Bragg rod data (Figure 6c, solid line).

Conclusion

This study presents an attempt to reveal the molecular arrangement of ionophores within a membrane-like environment. The unbound ionophores which form 3D crystals³ do not order at the air–water interface. The 2D crystallization of the complexed ionophores and their tendency to stack can be controlled by the lateral pressure, the presence of a matrix compound, and the type of counterions present in solution. The ordered films at the air–solution interface exhibit essentially similar packing as the 3D counterpart; however, some structural alternatives induced by the proximity to the solution interface may be detected by GID studies. These ordered forms of the ionophores might play diverse roles in the process of cation transport through membranes. The results described here provide incentive for applying these interface diffraction methods to artificial ion channels^{14,15} at interfaces.

Acknowledgment. This paper is dedicated to Professor Dieter Seebach on the occasion of his 60th birthday. The present work was supported by the Minerva Foundation (Munich, Germany), The Israel Academy of Basic Science and Humanity, the Danish Foundation for Natural Sciences, and Hasylab, DESY, Hamburg, Germany (for beam time).

JA971410Z

(14) Ghadiri, M. R.; Granja, J. R.; Milligan, R. A.; McRee, D. E.; Khazanovich, N. *Nature* **1993**, 366, 324.

(15) Matile, S.; Nakanishi, K. *Angew. Chem., Int. Ed. Engl.* **1996**, 35, 757.